Magnetic and electrical properties of Co/Si multilayer thin films

P. J. Grundy and J. M. Fallon*
Joule Physics Laboratory, University of Salford, Salford M5 4WT, United Kingdom

H. J. Blythe
Department of Physics and Astronomy, University of Sheffield, Sheffield S3 7RH, United Kingdom
(Received 24 March 2000)

This paper reports on the effects of interlayer mixing and a solid-state alloying reaction on the properties of a Co/Si multilayer system. The compositionally modified structure changes from a CoSi alloy to Co/CoSi to CoSi/Si layered systems as the nominal thickness of Si is increased over that of Co. The temperature-dependent magnetic properties of the multilayers are complex, with ferromagnetic and also thermally unstable superparamagnetic properties characterized by a blocking temperature behavior typical of small, low anisotropy particles. The electrical resistivity charts a transition from metallic to nonmetallic character as a function of increasing Si content. Resistivity minima and large magnetic saturation fields at low temperatures suggest the presence of Kondo-like behavior typical of dilute alloys.

I. INTRODUCTION

On alloying in equilibrium conditions the Co-Si binary system shows negative heats of mixing, which in sputter-deposited alloy thin films[1] encourage mutual solubility and the formation of extended alloy compositions and metastable amorphous phases. In multilayers this results in significant mixing at the layer interfaces and the formation of different microstructures and interlayer alloys of varying composition.[2] This paper reports on the temperature-dependent electrical resistivity and magnetic properties of such multilayers. We have varied the nominal Si-layer thicknesses with the intention of linking the observed magnetic and electrical properties to the microstructure of the multilayers[2] as the Si-layer thickness is varied.

Mixing at the interface of Co and Si layers has been interpreted in terms of ballistic mixing,[3] in which the transferred momentum of the depositing Co atoms allows them to penetrate the underlying Si layer. However, it is unlikely that typical adatom energies (<10 eV) are sufficient to cause the mixing observed in sputtered systems[4] and a chemical solid-state reaction (SSAR) is more likely. The diffusion of the slower diffuser, Si, through the interlayer is thought to be difficult and once formed the interface acts as a diffusion barrier.[5] Both evaporated[3] and sputtered[4] Co/Si multilayers show amorphous interlayers. High-resolution electron micrographs[4] have suggested that for small, nominal Co thicknesses (~ 3 nm) the metal is converted to an amorphous silicide with a fixed, average composition. Thicker Co layers can retain a part that is unalloyed, preserved by the diffusion barrier provided by the amorphous interlayer. Our recent results[2] generally support those findings, with the added observation of surprisingly uniform interlayers with an average composition that appears to depend on the relative, nominal thicknesses of the individual Co and Si layers. For relatively thin Co and Si layers ($\leqslant 5$ nm), elemental Co or Si may not be present and, instead, an alloy forms with an average composition that is, again, dependent on the relative thicknesses of the Co and Si layers. The interlayer thickness itself may also be controlled by the amount of deposited material made available to the reaction. It can also dilate as a result of a change from a crystalline to an amorphous state as the proportion of Si increases to above about 30 at. %, i.e., in the system reported on here, to a Si layer thickness greater than about 1 nm. For Si thicknesses below about 1 nm the multilayer is effectively a CoSi alloy polycrystal.

Fe/Si multilayers have shown[6] biquadratic antiferromagnetic coupling at Si thicknesses of between 0.8 and 1.6 nm. This interaction is temperature dependent and takes place between the iron layers via a nonmagnetic iron silicide interlayer.[7] The involvement of some form of charge carrier mechanism in supporting the strong remanent magnetization at low temperatures has also been invoked.[7] There was no detailed search for such a coupling in Co/Si multilayers in the work reported here, but measurements on multilayers with Si thicknesses between 0.6 and 1.8 nm did not reveal any strong evidence of such an effect.

Little attention has been paid to temperature-dependent electrical resistivity measurements on transition-metal/metalloid multilayers. The findings in this work are very reminiscent of the results obtained[8] for NiP alloy thin films as their structure changes from crystalline to amorphous with increasing metalloid content. Our results include a change in sign in the temperature coefficient of resistivity, resistivity maxima, and also Kondo-like resistivity minima as the Si content of the multilayers increases.

II. EXPERIMENT

Co/Si multilayer thin films were deposited on to Si wafer substrates using dc magnetron sputtering from separate Co and Si targets (of 99.99% purity) arranged in a cluster geometry. A single series of Co/Si multilayers having the nominal structure $(\mathrm{Co}2.2\,\mathrm{nm}/\mathrm{Si}\,X\,\mathrm{nm})_{12}$, where $0\ \mathrm{nm} < x < 9\ \mathrm{nm}$, was investigated. Sequential deposition was achieved using computer controlled shutters. The deposition system was maintained at a base pressure of 5×10^{-8} mbars and the samples were deposited at an Ar partial pressure of 1.6

$\times 10^{-2}$ mbars. The deposition rates were held fixed at 0.07 nm s^{-1} for Co and 0.03 nm s^{-1} for Si.

High angle x-ray diffraction and low angle x-ray reflectometry gave d spacings in the individual layers, the total thickness and the bilayer period of the multilayer structures. Microstructural features, both in cross section and plan view, and electron-diffraction patterns, were observed by high-resolution electron microscopy (TEM). Magnetic properties were measured in an alternating gradient force magnetometer (AGFM) at ambient temperatures and in a superconducting quantum interference device (SQUID) magnetometer at temperatures between 5 and 300 K and in fields up to 5 T. Electrical resistance measurements were made using a four-point probe system in a continuous flow He cryostat, also at temperatures between 5 and 300 K.

III. RESULTS AND DISCUSSION

A. Microstructure

The multilayers discussed here were prepared at higher sputtering pressures than those reported on previously.[2] The intention was to increase the degree of thermalization of the arriving adatoms in order to definitely encourage a SSAR mechanism in any resulting interlayer mixing, rather than a ballistic process. The x-ray reflectivity measurements, shown for a selection of the multilayers in Fig. 1, suggest a well-defined multilayer structure, although the Kiessig fringes are not very well defined in these structures, in contrast to the case of the multilayers deposited at lower sputtering pressures,[2] and only relatively weak second- and third-order Bragg maxima are observed. This information, plus the relatively rapid falloff of intensity in the curves, implies that the interfaces are rougher;[9] greater ad-atom mobility at lower sputtering pressures clearly promotes smoother interfaces.

The critical angle θ_c in x-ray reflectivity, i.e., the grazing angle at which the x rays are close to penetrating the surface of the sample in the critical external reflection condition, is directly related to the electron density in the sample, and therefore to the average mass density of the sample and the atomic number and concentrations of the constituent atoms. Critical angle measurements, Fig. 2, which correspond to a maximum in reflectivity, show that as the Si-layer thickness is increased, θ_c and hence the electron density of the system reduces, as expected, but also that the average density of multilayers with nominally thinner layers is greater than for systems with thicker layers but similar compositions. It is also clear that relative values of θ_c, calculated from a compositionally weighted average of atomic scattering factors, i.e., $(27t_{\mathrm{Co}}-14t_{\mathrm{Si}})/(27+14)$, where t represents the nominal thickness of the layers and 27 and 14 are the atomic numbers of Co and Si, only agree with measured values from multilayers with thick layers, in which the thickness of the mixed interfaces is relatively small. Figure 3 shows that the observed bilayer thickness is less than the nominal value and that these differences, and therefore the atomic mixing distances, are not very much different for structures deposited at low and high pressures and appear to be essentially pressure, i.e., deposition energy, independent. This result points to a SSAR mechanism in the mixing. Thicker Si layers allow the faster diffusing Co to travel further and reduce the bilayer period below the nominal period more effectively. Below

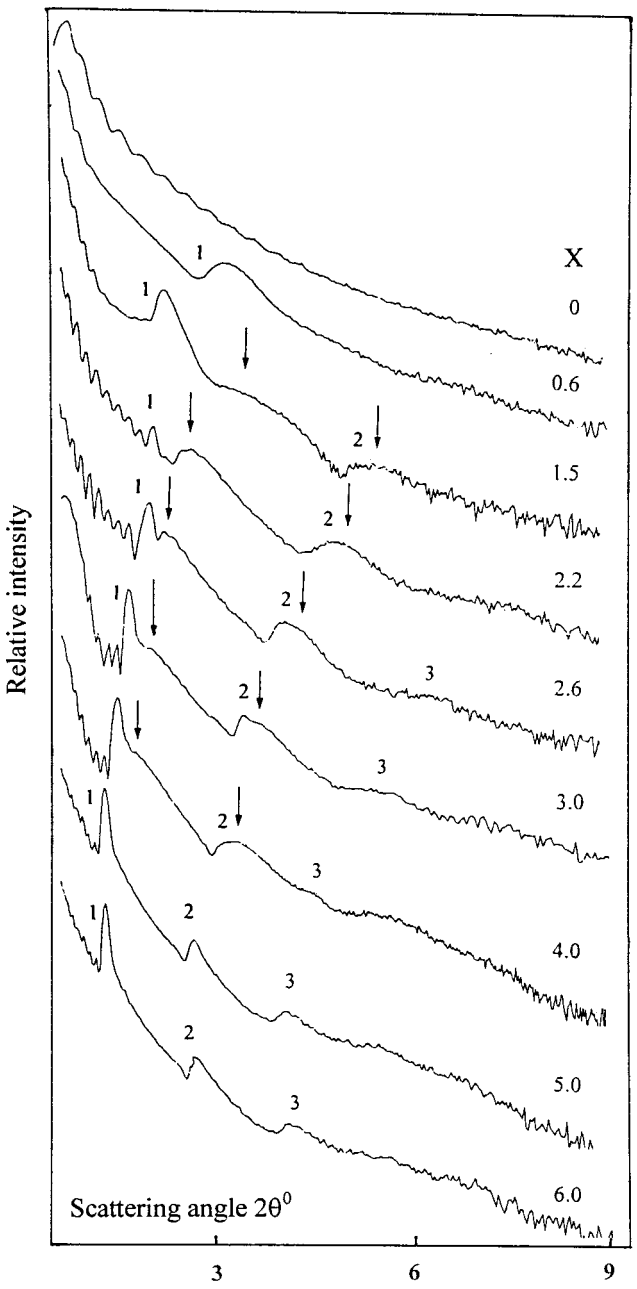

FIG. 1. X-ray reflectivity patterns for $(\mathrm{Co}\ 2.2\ \mathrm{nm/Si}\ X\ \mathrm{nm})_{12}$ multilayers displaced in X. The superimposed numbers mark Bragg maxima and the arrows the effect of a thin surface oxide.

layer thicknesses of ~2 nm there is much reduced electron and X-ray contrast between the layers. The cross-sectional high-resolution TEM micrograph in Fig. 4 of a $(\mathrm{Co}\ 2.2\ \mathrm{nm/Si}\ 1.2\ \mathrm{nm})_{12}$ multilayer on its Si/SiO_2 substrate shows this lack of contrast and what is the effective formation of a CoSi polycrystal with constant lattice fringe spacings up through the Co/Si stack, e.g., at x.

B. Magnetic properties

Normalized, ambient temperature AGFM magnetic hysteresis loops, Fig. 5, suggest that as Si is added to the structures the magnetization of the multilayer reduces. The magnetic character of the systems also changes from obvious ferromagnetism to what appears to be superparamagnetic be-

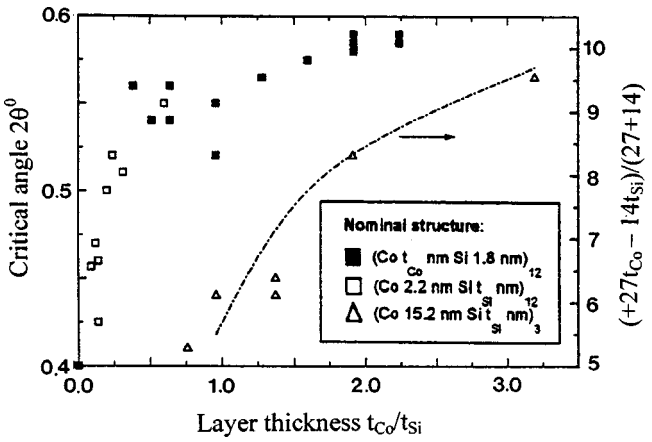

FIG. 2. A graph between the measured critical angle (actually $2\theta_c$) and a relative value of $2\theta_c$, calculated from a simple dilution law, plotted against the ratio of the nominal layer thicknesses $t_{\mathrm{Co}}/t_{\mathrm{Si}}$ of the multilayers. The open square symbols are for the samples discussed in this paper.

havior characterized by a canted loop, zero remanence, and much higher saturation fields. It is clear from the three loops shown that the transition from one type of magnetic behavior to the other is not abrupt but takes place gradually. As discussed in the Introduction, hysteresis loops gave no suggestion of antiferromagnetic coupling in the multilayers; the loss of remanence occurred at Si thicknesses above 4 or 5 nm.

Figure 6 shows SQUID measurements at 300 K of the effective Co moment in the samples. The moment decreases with increasing Si layer thickness from a value very near to that for bulk Co, at about $1.8\mu_B$, to very small values at Si-layer thicknesses greater than about 6 nm.

The apparent superparamagnetic behavior of the more diluted samples, i.e., more Si, suggested the investigation of field cooling measurements as a function of temperature. In such measurements a characteristic blocking temperature T_B can be defined above which the thermal relaxation time of the moments in the system is less than a reasonable observation time and the system behaves as a superparamagnet. Below T_B, the time scale for moment reversal is greater than the observation time and the system is seen as ferromagnetic. For clusters or particles of volume V and magnetic anisotropy K the blocking temperature is often defined by $25kT_B \sim KV$,[10,12] where k is the Boltzmann constant. Increasing the temperature of a sample, previously cooled in zero field (ZFC), in a small measuring field causes an increase in moment to the blocking temperature as thermal fluctuations increase and the probability of alignment of the moment increases. Above T_B, particles in the sample are superparamagnetic and the moment decreases again. The width of the blocking transition is related to a distribution of anisotropies or effective particle sizes. Cooling in the measuring field (FC) to complete the cycle causes the effective moment to increase. ZFC/FC curves, corrected for the influence of the substrate, made above and below the blocking temperature T_B are shown in Fig. 7. Corrected hysteresis loops measured at 5 and 300 K are shown in the insets.

The curves for $x=0$ in Fig. 7(a) show no bifurcation, as expected for a ferromagnetic Co thin-film sample. The inset loops are clearly ferromagnetic in character at both the low-

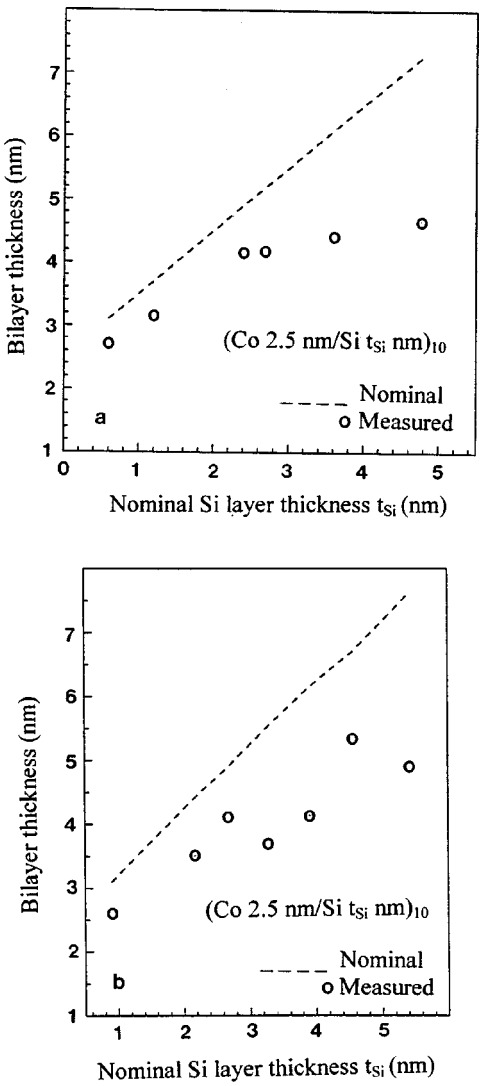

FIG. 3. Nominal and measured bilayer thicknesses plotted against the nominal Si layer thickness for two similar multilayer series deposited at different sputtering pressures (a) 4×10^{-3} mbars and (b) 16×10^{-3} mbars.

est temperature and at 300 K. The first feature to note in Figs. 7(b) and (c) is the presence of a blocking transition in the ZFC curves and the reduction in the temperature of the transition maximum (T_B) as the Si-layer thickness, i.e., the Si content of the multilayer, increases. This is most probably a result of the formation of thermally unstable and low anisotropy amorphous particles. The second point is the change in width of the transition. For structures around the percolation threshold (~50 at. % Si), e.g., (Co 2.2 nm/Si 3.0 nm)$_{12}$, quite a broad blocking distribution is found but beyond the percolation threshold, e.g., at Si thicknesses of 6 and 9 nm, the barrier distribution narrows. The blocking temperature reduces progressively from ~150 K for 3 nm of Si to ~14 K for 9 nm of Si. This trend can be understood as a gradual dilution of the Co layers. A similar trend has been repeatedly found[11] with sputter co-deposited granular Co-Ag alloys as the Ag fraction is increased.

Despite the large changes in T_B, particle sizes, as measured by TEM, were found not to change much with Si composition, implying that compositional differences between

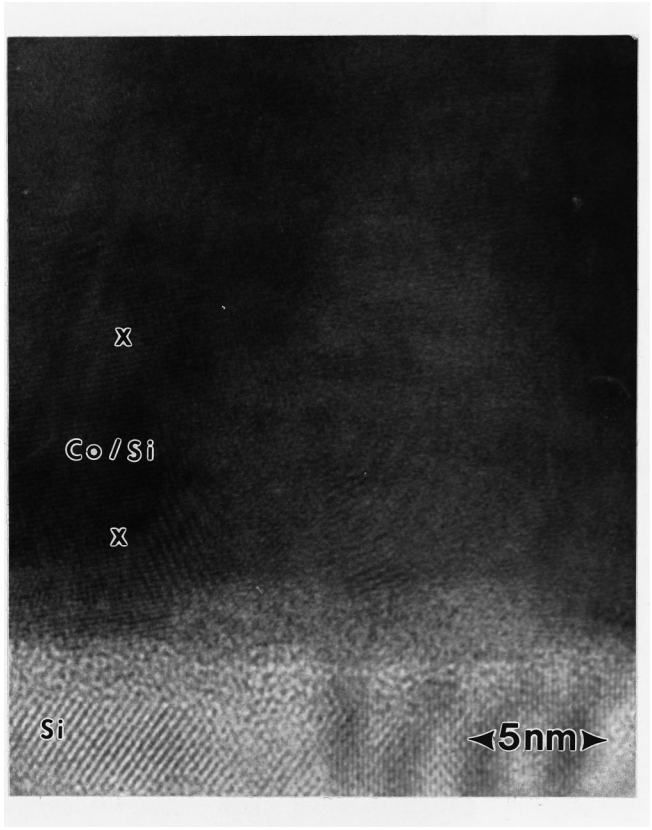

FIG. 4. Cross-sectional high-resolution TEM micrograph of a $(\mathrm{Co\ 2.2\ nm/Si\ 1.2\ nm})_{12}$ multilayer showing the growth of large crystalline grains up through the layer stack from the Si/SiO_2 substrate.

samples and concomitant changes in anisotropy are important. These changes occur by a dilution and associated amorphization of the Co layers. Average particle or grain diameters were measured for the samples and, using the Livingston and Bean expression[12] anisotropy values were calculated, Table I. They are surprisingly large, especially for amorphous particles that have no long-range crystalline order. Values for hcp Co (K_1) are $\sim 4\times 10^5\ \mathrm{J\,m^{-3}}$,[13] and for amorphous systems they are usually of the order of $10^4\ \mathrm{J\,m^{-3}}$.[14] The gradation in values here is consistent with a crystalline to amorphous transformation through the multilayer series. Figure 8 shows a plan view TEM micrograph and plan view electron-diffraction pattern for $x = 1.8\ \mathrm{nm}$, in which there are the clear beginnings of a transition from a typical hcp diffraction pattern to an amorphous pattern and the loss of regular lattice fringes in the granular-like regions in the micrograph. The high values of anisotropy indicate a contribution from any remaining crystalline Co or other important sources of anisotropy, or the measured TEM particle diameters do not properly represent the effective magnetic particle size; this is possible since the dark particles in Fig. 8(a) are in close contact. The hysteresis loops measured at 5 K for the thicker Si-layer samples, e.g., Fig. 7(c), display higher saturation fields that may indicate a coexisting paramagnetic phase, as found with Co-Pd-Si.[15]

It was anticipated that thicker Si layers would produce the largest changes in H_c with temperature. This is because the formation of thermally unstable particles should be more efficient and thus allow the number fraction of initially noncoercive, irreversible particles to increase substantially with reducing temperature. Instead, all the multilayers show similar changes in magnitude. Films were often coercive above T_B, with the exception of $(\mathrm{Co\ 2.2\ nm/Si\ 9.0\ nm})_{12}$. For uniaxial single domain particles, coercivity H_c can be written as[12]

$$H_c = \frac{2K}{M_S}\left\{1-\left(\frac{25kT}{KV}\right)^{1/2}\right\}. \tag{1}$$

This is close to the ideal Stoner-Wolhfarth value of $2\,K/M_s$ only for lowest temperatures and disappears on increasing the temperature to T_B. The coercivity, below the blocking temperature, should yield a straight line when plotted as $1-(T/T_B)^{1/2}$ if single domain particles are present. Results plotted in this fashion, Fig. 9(a), show a departure from the straight line, attributable to a possible temperature dependence of the anisotropy. The temperature at which the curves

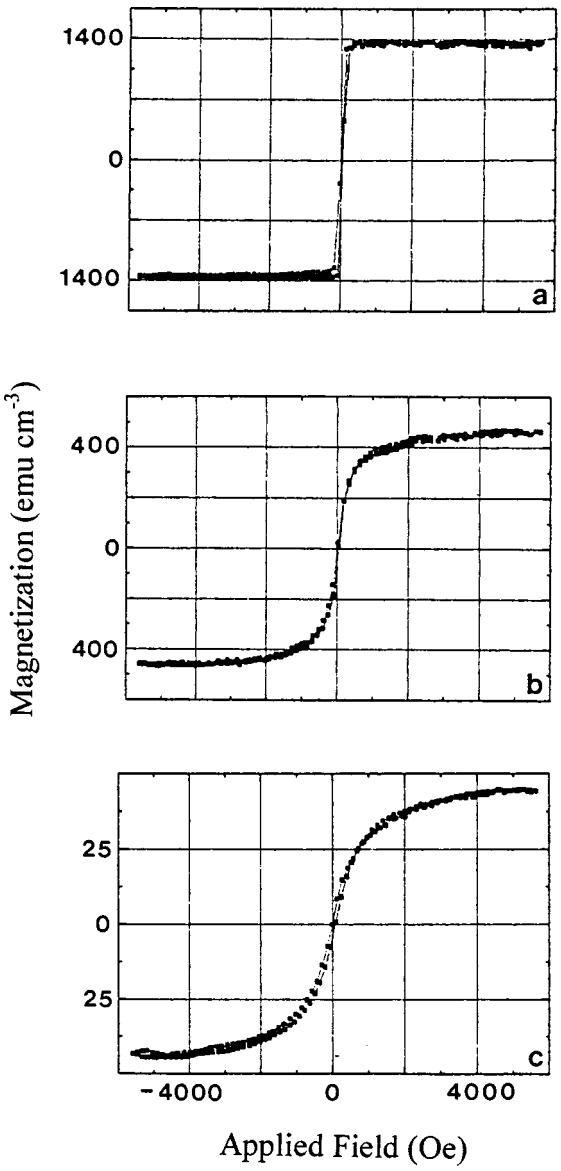

FIG. 5. AGFM magnetic hysteresis loops at ambient temperature (~295 K) for $(\mathrm{Co\ 2.2\ nm/Si}\ X\ \mathrm{nm})_{12}$ multilayers, (a) $X=0$, (b) $X=5.0$, and (c) $X=8.5\ \mathrm{nm}$. Magnetization values are per unit volume of Co.

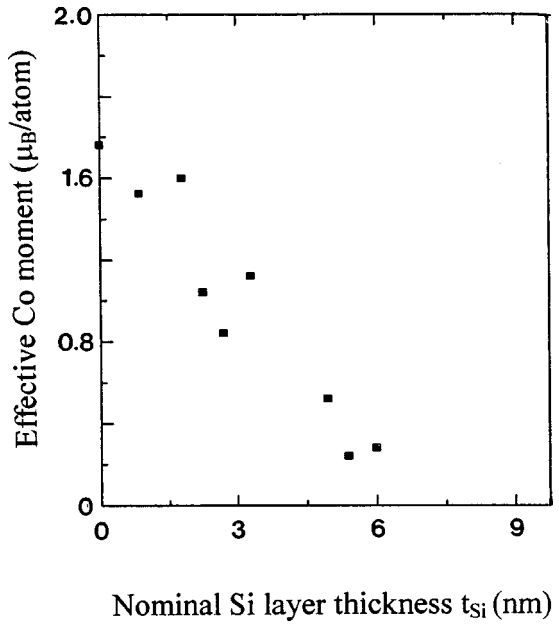

FIG. 6. A plot of the effective moment on the Co ions for $(\mathrm{Co}\ 2.2\ \mathrm{nm/Si}\ X\ \mathrm{nm})_{12}$ multilayers as a function of the Si-layer thickness.

deviate from linearity approximates very roughly to the blocking temperature, at least for the system with thicker layers, as marked.

Normalized remanence measurements, obtained from hysteresis loops measured up to 1 T are summarized in Fig. 9(b). As temperature is increased, thermal energy allows moments to become unstable and causes the remanence to decrease, reaching zero close to T_B for most of the samples, as for a superparamagnet. $M_r/M_s \sim \frac{1}{2}$ at low temperature is taken as a signature for isolated, uniaxial single-domain particles. For the samples here, values are in this region only for $(\mathrm{Co}\ 2.2\ \mathrm{nm/Si}\ 9.0\ \mathrm{nm})_{12}$. A similar trend has been observed in granular Co/Re alloy thin films on increasing the Re content.[16]

The initial susceptibility, obtained from the FC measurements as in Fig. 10, follows a linear $1/\chi$ versus T Curie-Weiss law as for a paramagnet. The sample with the thickest Si layer $(\mathrm{Co}\ 2.2\ \mathrm{nm/Si}\ 9.0\ \mathrm{nm})_{12}$ has the best fit, but at lower T a deviation occurs resulting in the curve for this sample not passing near to the origin. Extrapolating the straight line region at higher T gives an intercept of 25 K, which is close to T_B for this sample. This is supportive of the blocking hypothesis because samples with less Si show a stronger departure from Curie-Weiss behavior as T_B is approached.

With superparamagnetism all measurements of moment made above T_B when plotted as M vs H/T should fall on the same curve. This is best obeyed for the samples with the thicker 6- and 9-nm Si layers. Figure 11 shows the results for the 6-nm case. The cluster size can be indirectly estimated from the average moment, μ_{eff} of the cluster. An attempt at this was made by fitting the Langevin function $M(H)$ to the reduced field H/T curves above T_B and by assuming that particles are noninteracting and of uniform size. The solid curve represents $L(\alpha)$ corresponding to $\mu_{\mathrm{eff}} \sim 15\,000\mu_B$. Assuming the average effective moment of Co atoms in the 6-nm Si multilayer to be $0.2\mu_B$, as shown in Fig. 6, and a

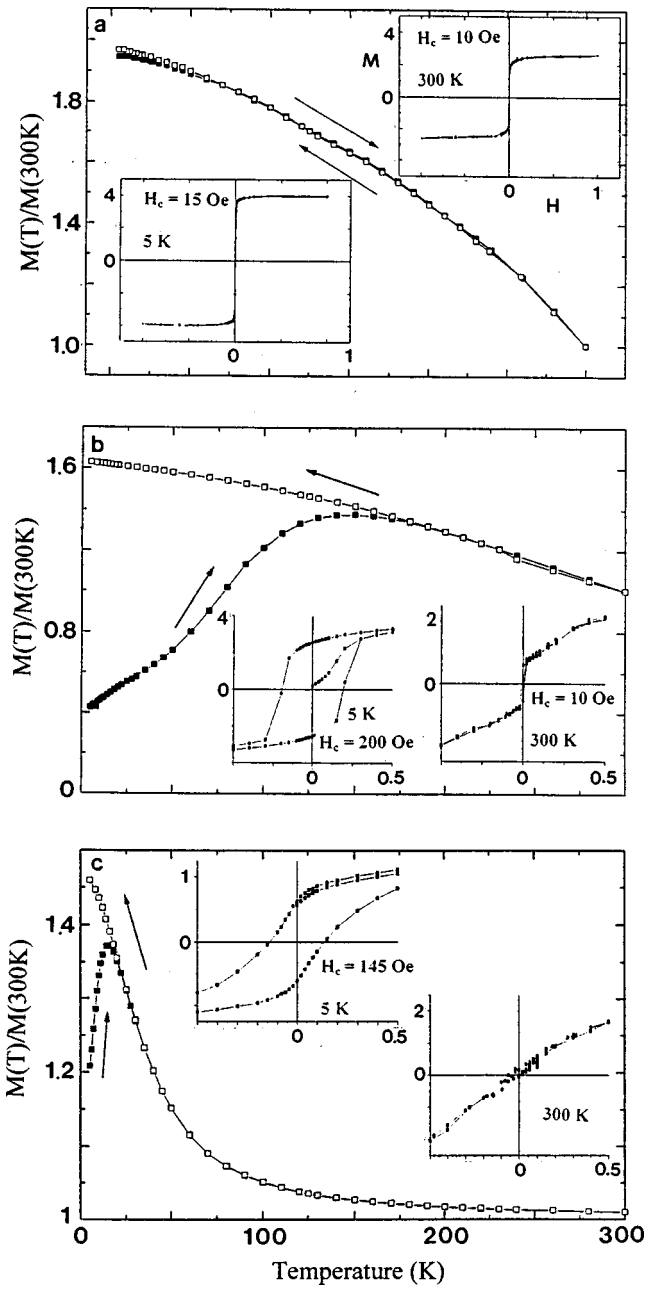

FIG. 7. ZFC/FC curves for the multilayers with (a) $X=0$, (b) $X=3$, and (c) $X=9$ nm. The curves with solid squares are for samples initially cooled in zero magnetic field (ZFC) and the curves with hollow squares are for samples cooled in the measuring field of 5 mT (FC). The inset hysteresis loops give the coercivity and the temperature of measurement. The moments are multiples of 10^{-4} emu and the applied fields are in kOe.

spherical cluster with atoms each of effective radius 0.1 nm, a particle diameter of 6 nm is calculated; a value close to that given in Table I.

C. Thermal electrical resistivity measurements

Detailed reports of the temperature dependence of the electrical resistivity of transition-metal-metalloid combinations are confined to a limited number of alloys prepared by co-deposition.[8,17] The data plots, for samples from this research, Fig. 12, show the value of the reduced resistivity at

TABLE I. Effective anisotropy values assuming particle diameters from TEM measurements.

Nominal structure $(\text{Co } 2.2\text{ nm/Si } X\text{ nm})_{12}$ X	Blocking temperature T_B K	Average particle diameter nm	Effective anisotropy $\times 10^5$ J m^{-3}
1.8	~320	8.0	4.6
3.0	147	5.8	5.4
3.6	97	6.1	3.6
6.0	16	5.2	1.3
9.0	14	5.1	0.7

temperature T, normalized for convenience to that at 225 K, for several Co/Si multilayers each with a different nominal Si-layer thickness. They chart a transition from metallic to nonmetallic behavior. The resulting resistivity changes, though small, are comparable in magnitude with those observed for Ni-P alloys.[8]

The metallic conduction of the Co layers, typified by a $\rho \propto T^n$ relationship, as in Fig. 12, is broken by a dilution of the Co layers by Si through mixing or by the formation of partially insulating barriers. However, resisitivities are not so high as to suggest conduction by a hopping mechanism; the metal-insulator transition in Co-Si alloys occurs around about 15 at. % Co.[18] Changes in the temperature coefficient of resistivity, α (225 K), i.e., the slope in the curves at 225 K of Fig. 12, as Si is added also indicate amorphization of the initial crystalline Co layers by combination with Si. The compositional modulation period itself may not have much of an impact on the ρ-T curves since mean free paths in most amorphous metallic samples are of the order of the atomic spacing.

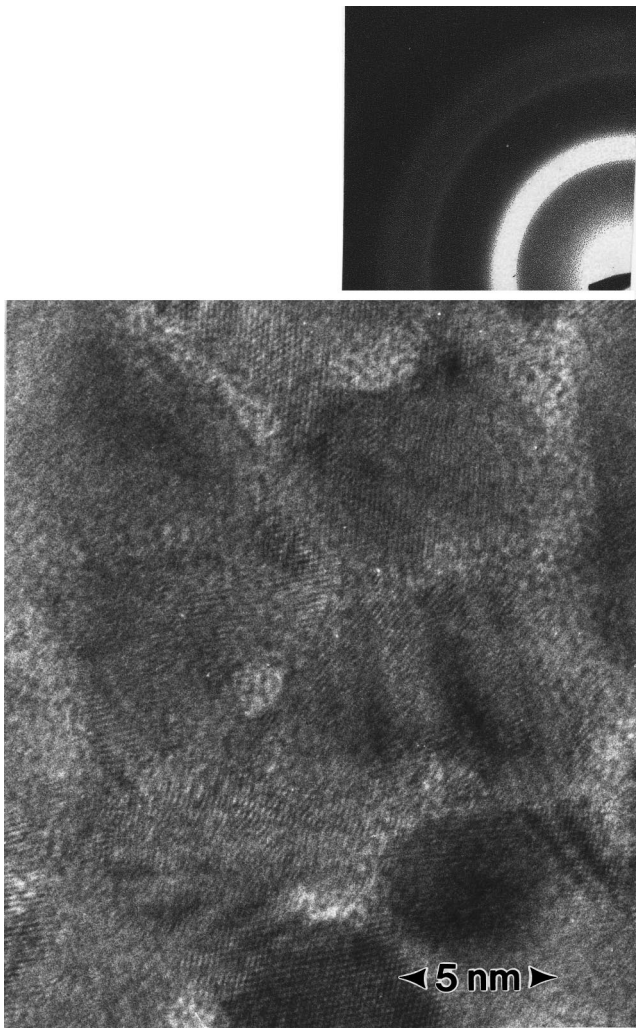

FIG. 8. Plan view TEM micrograph and electron-diffraction pattern for a multilayer with $X = 1.8$ nm.

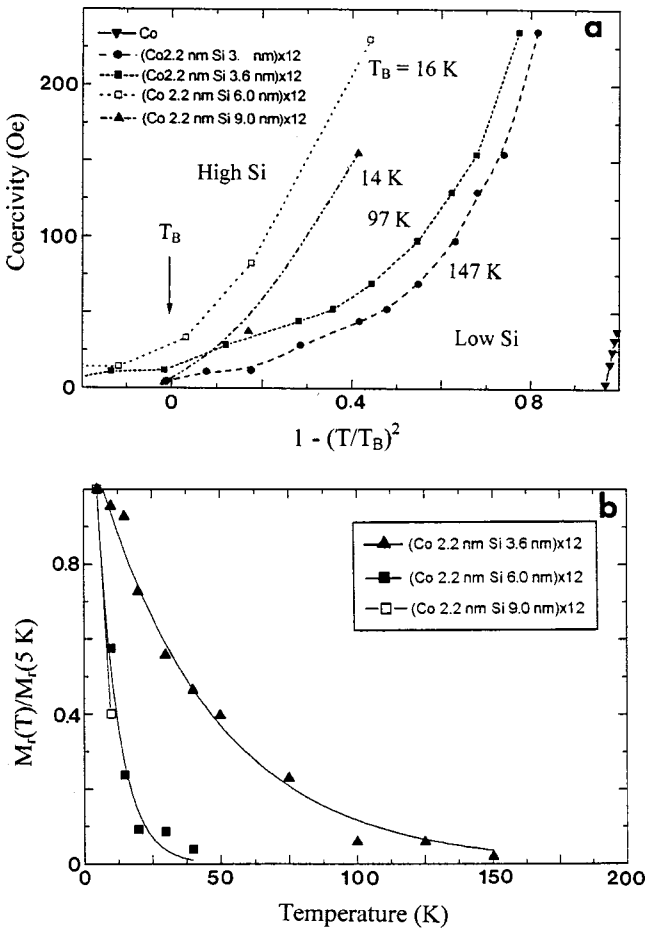

FIG. 9. Tests for single domain behavior with (a) a plot of coercivity against reduced temperature and (b) reduced remanence against temperature.

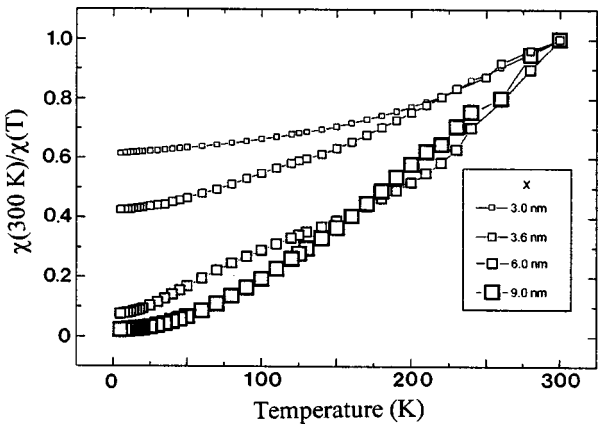

FIG. 10. A plot of inverse susceptibility $1/\chi$ as $\chi(300\text{ K})/\chi(T)$ against temperature for the multilayers with the thicker Si layers.

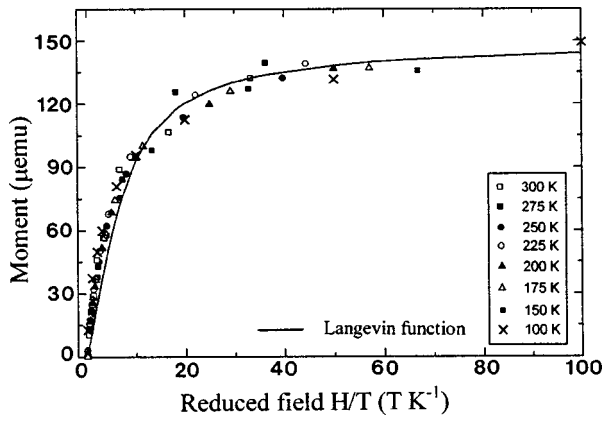

FIG. 11. Magnetic moment versus the reduced field for the $(\text{Co } 2.2\text{ nm/Si } 6\text{ nm})_{12}$ multilayer.

Measurements above and below 75 K will be discussed separately as this temperature marks a distinct change in the ρ-T behavior. Above 75 K, samples with nominal Si thicknesses below 1.0 nm show a positive slope in the resistivity versus temperature curve at 225 K (as at 300 K also). This positive temperature coefficient of resistivity and the small residual resistivity (compare to the value for pure Co, $\rho_0 = 5.86\,\mu\Omega$ cm) are features typical of crystalline metallic films.

For the multilayer with a nominal Si thickness of 1.5 nm, and a co-deposited amorphous alloy,[1] included as a comparison, the residual resistivity contribution becomes more substantial and the resisitivity is weakly temperature dependent, as usual for structurally disordered alloys. Small positive or negative values of α are typical of amorphous metal-metalloids,[19] and suggest that the predominant part of the scattering is due to the disordered atomic arrangement.

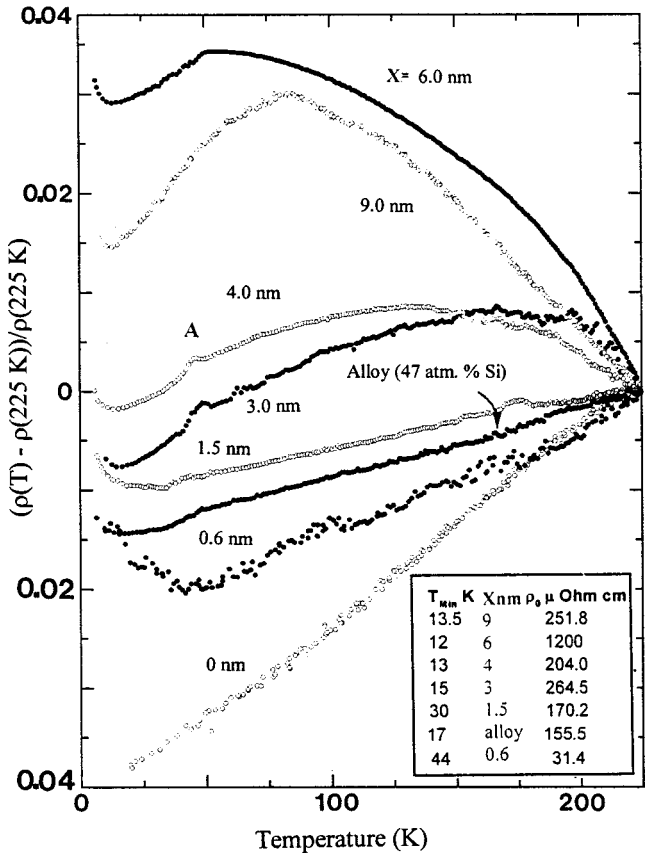

FIG. 12. The normalized resistivity difference against temperature for the $(\text{Co } 2.2\text{ nm/Si } X\text{ nm})_{12}$ multilayers and a $Co_{53}Si_{47}$ alloy. The temperatures of the resistivity minima $T_{\min}$, X, and the residual resistivities ρ_0 are given inset.

With Si thicknesses greater than 2.0 nm, the residual resistivity increases further: the inherent structural disorder increases and a change in sign of α at higher temperatures causes the resistivity to pass through a maximum. Increasing the nominal Si-layer thickness further to ~6-nm shifts this maximum to lower temperatures, while increasing the residual resisitivity. The movement of the broad maximum in the curves to lower temperatures, as Si is added, is not consistent with any change in magnetic property but is, however, consistent with the structural localization idea.[19] Small phonon vibrations at low temperature are capable of effectively limiting the mean free path in highly disordered structures which encourages localization. With less disordered structures larger phonon vibrations at higher temperatures are needed to produce a saturation in the resistivity. Alternatively, resistivity can drop with increasing temperature since localization of conduction electrons leads to bound states from which electrons can be thermally excited.[20] However, this effect could also be related to the temperature dependence of the structure factor and valency effects.[21]

At temperature below 75 K, the resistivity/temperature relationship changes to a $\rho \propto T^2$ behavior[22] with increasing Si thickness. The layered structures, and, to some extent, the alloy, all show an anomalous increase in resistivity with decreasing temperature at very low temperatures. This produces a temperature resistivity minimum, e.g., at ~44 K for 0.6 nm of Si, as for other disordered alloys containing magnetic transition ions.[23] The minimum moves toward lower temperatures as the Si-layer thickness is increased. The appearance of the resistivity minimum, at a low residual resistivity ($\rho_0 \sim 30\,\mu\Omega$ cm) for 0.6 nm Si, its presence at higher values ($\rho_0 = 1200\,\mu\Omega$ cm) for thicker Si, but its absence in the Co film, suggests that it is the presence of randomly isolated Co ions that is important in producing the minimum. Such ions rely on the natural random nature of the amorphous phase for their existence.[23] The average structure over the volume of the multilayer itself (whether Co is dissolved in a random Si tetrahedral network or it forms a single phase, dense randomly packed alloy) does not seem to be of consequence. This perhaps supports the idea that random isolated magnetic ions are indeed important in the causing the resistivity upturn on moving to the lowest temperatures.

In some of the strongly disordered structures, ρ-T curves appear to show a particular feature, as marked at ''A'' in Fig. 12, at the crossover from a linear to a quadratic temperature behavior. This is not reported in the literature for any metal-metalloid combination. Its origin is not an artifact of the experiment but could be related to some magnetic scattering, though certainly not to a blocking transition. Its discreteness and the fact that it does not change with temperature would suggest that it may be electronic in origin.

Since all the events discussed here are analogous to those found with metallic glasses, formed by alloying a transition metal T with a metalloid element M, particularly the studies of $Ni_{1-X}P_X$,[8] and $(\text{Pd-Ni})_{1-X}P_x$,[24] where $X \sim 0.2-0.3$, it is

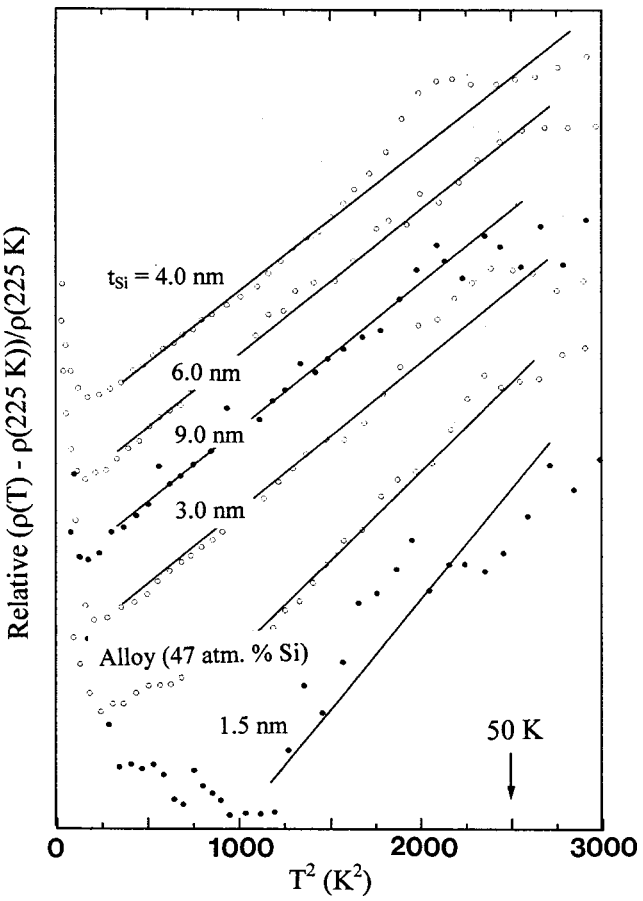

FIG. 13. The normalized resistivity difference versus the square of the temperature. The curves are displaced for visibility.

interesting to inquire whether multilayers with compositions in the range $T_{0.7-0.8}/M_{0.3-0.2}$ also show the same effects. For example, electron conduction in these Co/Si multilayers will follow the paths of lower resistance which will be expected to have a composition different to that of the average of the bulk film. Unfortunately, a series of measurements as in Fig. 12, is unavailable for co-deposited Co-Si alloys. Comparing with Ni-P alloys, though, it can be said that comparatively less Co is needed with Si than for Ni in Ni-P to produce similarly shaped resistivity/temperature curves.

At low temperatures all samples are mainly ferromagnetic, but the large saturation field at 5 K derives from either the amorphous structure in the multilayers containing the larger Si thicknesses and/or from a number of isolated paramagnetic Co ''impurity'' ions that allow a Kondo scattering mechanism, as for Pd-Co-P (Ref. 25) or Pd-Co-Si alloys.[23] The theory behind this magnetic scattering, rather than the structural model,[26] can be applied to the data in Fig. 12. To test whether the Kondo mechanism, strictly applicable to dilute magnetic alloys, is responsible, the equation

$$\rho_{\text{total}} = \rho_0 - \rho_{\text{Kondo}} + bT^2, \tag{2}$$

where

$$\rho_{\text{Kondo}} = c\rho_M \left[1 + \frac{3ZJ}{E_F} \ln T \right], \tag{3}$$

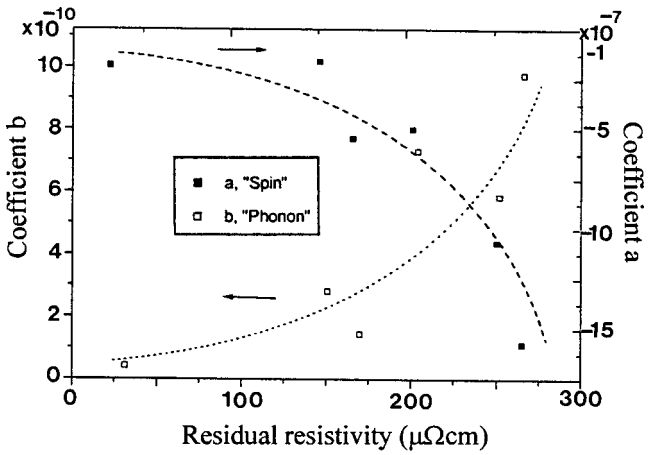

FIG. 14. The values of the parameters a and b plotted against the residual resistivity.

allows a phenomenological derivation of the temperature minimum. Here c is the concentration of any paramagnetic ions, Z is the valency of the $3d$ ion, ρ_M is a measure of the strength of the exchange scattering, and J is the exchange interaction energy between the spin of the $3d$ ion and that of the surrounding conduction electrons. The minima T_{min} in the transitions in Fig. 12 are similar in form to those observed in paramagnetic Ni-P alloys.[8] Although the magnetic measurements indicate that all samples in this work are ferromagnetic at temperatures less than 30 K, the resistivity fits are best for a T^2 (electron-phonon) rather than a $T^{3/2}$ (electron-magnon) behavior in the temperature range 5–50 K, Fig. 13.

For temperatures less than 50 K, where the term for the assumed Kondo mechanism is operative, the parameters ρ_0 and b in the above equation can be determined from Fig. 13 and then a, a term containing the parameters multiplying the $\ln T$ term in Eq. (3), can be calculated. Values of a, b, and ρ_0 are plotted in Fig. 14. The coefficient a is proportional to the exchange interaction $J_{s\text{-}d}$ between the spin of the magnetic atom and that of the conduction electrons and is seen to decrease as the Si layer is made thicker and ρ_0 increases. The predictions for T_{min} using Eqs. (2) and (3), i.e., $T_{\text{min}} = (a/2b)^{1/2}$, is plotted in Fig. 15 alongside experimental mea-

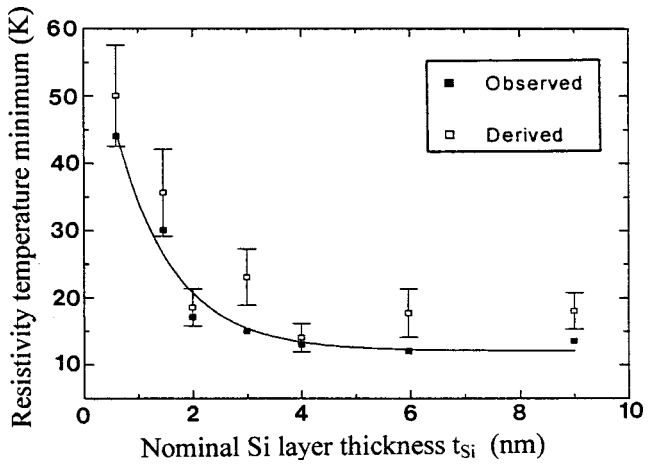

FIG. 15. Values of the experimental and derived resistivity minima plotted against the nominal Si-layer thicknesses.

surements for all samples studied. The agreement with experimental T_{min} is within estimated error, supporting a Kondo-type scattering mechanism.

IV. CONCLUSION

The aim of the investigation reported herein was to correlate the features of interlayer mixing in a multilayer film composed of a ferromagnetic transition metal and a nonmetallic and nonmagnetic spacer layer with the magnetic and electrical properties of the system. The Co/Si interface exhibits such extensive mixing that with thin ($\leqslant$5 nm) nominal layers, completely elemental layers cannot form and the system is compositionally modulated with, probably, a transition from a CoSi alloy to Co/CoSi to CoSi/Si multilayers as the nominal thickness of Si is increased over that of Co. The average composition of the system depends on the designed layer thicknesses. It is found that with increasing Si-layer thicknesses, and the increasing effect of the interlayer diffusion of the Co, that the systems become essentially amorphous.

The temperature-dependent magnetic properties of the multilayers exhibit a complex behavior, with ferromagnetic and also thermally unstable superparamagnetic characteristics. The superparamagnetic situation is characterized by typical blocking temperature behavior and is interpreted in terms of the effective formation of small particles with low anisotopies. The electrical resistivity charts a transition from metallic to nonmetallic behavior as a function of increasing Si content. Minima in resistivity and large magnetic saturation fields at low temperatures suggest Kondo-like behavior typical of dilute alloys.

*Present address: DERA, St. Andrew's Road, Great Malvern, WR14 3PS, UK.

[1] J. M. Fallon, C. A. Faunce, and P. J. Grundy, J. Phys.: Condens. Matter **12**, 4075 (2000).
[2] J. M. Fallon, C. A. Faunce, and P. J. Grundy, J. Appl. Phys. **88**, 2400 (2000).
[3] A. K. Petford-Long, M. B. Stearns, C. H. Lee, S. R. Nutt, M. Ceglio, and A. M. Hawryluk, J. Appl. Phys. **61**, 1422 (1987).
[4] P. Ruterana, P. Haudy, and P. Boher, J. Appl. Phys. **68**, 1033 (1990).
[5] K. Holloway and R. Sinclair, J. Appl. Phys. **61**, 1359 (1987).
[6] J. Kohlepp, F. J. A. den Broeder, M. Valkier, and A. van der Graaf, J. Magn. Magn. Mater. **165**, 431 (1997).
[7] J. A. Carlisle, A. Chaiken, R. P. Michel, and L. J. Terminello, Phys. Rev. B **53**, R8824 (1996).
[8] P. J. Cote, Solid State Commun. **18**, 1311 (1976).
[9] J. M. Slaughter, D. W. Schulze, C. R. Hills, A. Mirone, R. Stalio, R. N. Watts, C. Tarrio, K. Kromrey, P. Mueller, and C. M. Falco, J. Appl. Phys. **76**, 2144 (1994).
[10] S. H. Charap, P-L Lu, and Y. He, IEEE Trans. Magn. **33**, 978 (1997).
[11] E.g., F. Conde, C. Gomez-Polo, and A. Hernando, J. Magn. Magn. Mater. **138**, 123 (1994).
[12] B. D. Cullity, in *Introduction to Magnetic Materials*, edited by M. Cohen (Addison-Wesley, New York, 1972).
[13] J. D. Sievert and V. Zehler, Z. Angew. Phys. **30**, 251 (1970).
[14] K. Moorjani and J. M. D. Cooey, in *Magnetic Glasses* (Elsevier, New York, 1984).
[15] M. E. Weiner, Ph.D. thesis, California Institute of Technology, 1978.
[16] G. A. Jones, C. A. Faunce, D. Ravinder, H. J. Blythe, and V. M. Fedosyuk, J. Magn. Magn. Mater. **184**, 28 (1998).
[17] G. Busch and H. Guntherodt, J. Solid State Chem. **29**, 235 (1975).
[18] M. M. Collver, Solid State Commun. **23**, 333 (1977).
[19] J. H. Mooij, Phys. Status Solidi A **17**, 521 (1973).
[20] N. Sharma, Ph.D. thesis, University of Bombay, 1987.
[21] S. R. Nagel, Phys. Rev. B **16**, 1694 (1977).
[22] F. J. Okhawa, J. Phys. Soc. Jpn. **44**, 1105 (1978).
[23] R. Hasegawa and C. C. Tsuei, Phys. Rev. B **3**, 214 (1971).
[24] B. Y. Bucher, J. Non-Cryst. Solids **72**, 277 (1972).
[25] N. I. Marzell, J. Magn. Magn. Mater. **5**, 67 (1977).
[26] R. W. Cochrane, R. Harris, J. O. Strom-Olsen, and M. J. Zuckerman, Phys. Rev. Lett. **35**, 676 (1975).